Roughness as a Route to the Ultimate Regime of Thermal Convection

Srikanth Toppaladoddi, Sauro Succi, and John S. Wettlaufer

Phys. Rev. Lett. **118**, 074503 — Published 16 February 2017

DOI: 10.1103/PhysRevLett.118.074503

Roughness as a Route to the Ultimate Regime of Thermal Convection

Srikanth Toppaladoddi,[1] Sauro Succi,[2] and John S. Wettlaufer[1,3,4]

[1] *Yale University, New Haven, Connecticut, USA*
[2] *Istituto per le Applicazioni del Calcolo "Mauro Picone" (C.N.R.), Rome, Italy*
[3] *Mathematical Institute, University of Oxford, Oxford, UK*
[4] *Nordita, Royal Institute of Technology and Stockholm University, Stockholm, Sweden[*]*

(Dated: December 19, 2016)

We use highly resolved numerical simulations to study turbulent Rayleigh-Bénard convection in a cell with sinusoidally rough upper and lower surfaces in two dimensions for $Pr = 1$ and $Ra = \left[4 \times 10^6, 3 \times 10^9\right]$. By varying the wavelength λ at a fixed amplitude, we find an optimal wavelength $\lambda_{\rm opt}$ for which the Nusselt-Rayleigh scaling relation is $\left(Nu - 1 \propto Ra^{0.483}\right)$ maximizing the heat flux. This is consistent with the upper bound of Goluskin and Doering [1] who prove that Nu can grow no faster than $\mathcal{O}(Ra^{1/2})$ as $Ra \to \infty$, and thus the concept that roughness facilitates the attainment of the so-called ultimate regime. Our data nearly achieve the largest growth rate permitted by the bound. When $\lambda \ll \lambda_{\rm opt}$ and $\lambda \gg \lambda_{\rm opt}$, the planar case is recovered, demonstrating how controlling the wall geometry manipulates the interaction between the boundary layers and the core flow. Finally, for each Ra we choose the maximum Nu among all λ, and thus optimizing over all λ, to find $Nu_{\rm opt} - 1 = 0.01 \times Ra^{0.444}$.

The ubiquity and importance of thermal convection in many natural and man-made settings is well known [2–4]. The simplest scenario that has been used to study the fundamental aspects of thermal convection is the Rayleigh-Bénard system [5]. The flow in this system is governed by three non-dimensional parameters: (1) the Rayleigh number $Ra = g\alpha\Delta T H^3/\nu\kappa$, which is the ratio of buoyancy to viscous forces, where g is the acceleration due to gravity, α the thermal expansion coefficient of the fluid, ΔT the temperature difference across a layer of fluid of depth H, ν the kinematic viscosity (or momentum diffusivity) and κ the thermal diffusivity; (2) the Prandtl number, $Pr = \nu/\kappa$; and (3) the aspect ratio of the cell, Γ, defined as the ratio of its width to height.

The primary aim of the corpus of studies of turbulent Rayleigh-Bénard convection has been to determine the Nusselt number, Nu, defined as the ratio of total heat flux to conductive heat flux (Eq. 1), as a function of the three governing parameters, viz., $Nu = Nu(Ra, Pr, \Gamma)$. For $Ra \gg 1$ and fixed Pr and Γ, this relation is usually sought in the form of a power law: $Nu = A(Pr, \Gamma) Ra^{\beta}$, where β has a fundamental significance for the mechanisms underlying the transport of heat.

The classical theory of Priestley [6], Malkus [7] and Howard [8] is based on the argument that as $Ra \to \infty$ the dimensional heat flux should become independent of the depth of the cell, resulting in $\beta = 1/3$. A consequence of this scaling is that the conductive boundary layers (BLs) at the upper and lower surfaces, which are separated by a well mixed interior, do not interact.

However, Kraichnan [9] reasoned that for extremely large Ra the BLs undergo a transition leading to the generation of smaller scales near the boundaries that increase the system's efficiency in transporting the heat, predicting that $Nu \sim \left[Ra/\left(\ln Ra\right)^3\right]^{1/2}$. In this, "Kraichnan-Spiegel" or "ultimate regime" ($\beta = 1/2$), it is argued that the heat flux becomes independent of the molecular properties of the fluid [e.g., 10, 11]. Experimental [12–15] and numerical [16–18] studies have found $\beta \approx 1/3$. Chavanne *et al.* [19] and He *et al.* [20] have reported observing transitions to $\beta = 0.39$ and $\beta = 0.38$ in their respective experiments and these findings continue to stimulate discussion [21, 22]. Motivated by studies of shear flow, Borue and Orszag [23] used pseudo-spectral methods at three resolutions (64^3, 128^3, 256^3 and hence values of Ra) to study "homogeneous" convection, in which the BL's are effectively removed. Whilst the highest resolution was not numerically converged, the other two resolutions led to a range of $\beta = 0.40 \pm 0.05$. This idea was later used in Lattice Boltzmann simulations for $Ra = \left[8.64 \times 10^5, 1.38 \times 10^7\right]$, to find $\beta = 0.51 \pm 0.06$ [24], ascribing this to the ultimate regime.

Recently, Waleffe *et al.* [25] and Sondak *et al.* [26] numerically computed the steady solutions to the Oberbeck-Boussinesq equations for $Ra \le 10^9$ and $1 \le Pr \le 100$ in two dimensions. By fixing Ra and Pr, steady solutions for different horizontal wavenumbers, α, were computed. The solution that maximized heat transport, $Nu \equiv Nu_{opt}$, was called optimal, for which $\alpha \equiv \alpha_{opt}$ and $Nu_{opt} - 1 = 0.115 \times Ra^{0.31}$, which is in agreement with experiments [12]. Although they found that β was independent of Pr, the Prandtl number did have considerable effect on the geometry of the coherent structures that transported heat. For $Pr > 7$, the scaling for the optimal wavenumber was found to be $\alpha_{\rm opt} = 0.257 \times Ra^{0.256}$. The horizontally averaged optimal temperature profiles had the following features: (a) The BLs were always unstably stratified. (b) The core region was either stably ($Pr \le 7$) or unstably ($Pr > 7$) stratified. (c) The transition regions between the core and BLs were always stably stratified. Thus, with small departures, these profiles correspond to the marginally stable profile of Malkus [7], with $\beta = 1/3$.

An important aspect emerging from the study of planar Rayleigh-Bénard convection in two dimensions for $Pr \geq 1$ is that the flow field [27] and the Nu-Ra scaling relations [25, 26, 28] are similar to those in three dimensions. Thus, this correspondence permits one to understand the processes driving the heat transport using well resolved two-dimensional simulations.

It is clear that the value β takes in the limit $Ra \to \infty$ depends on the interaction between the BLs and the core flow. To understand the role of BLs in thermal convection, Shen *et al.* [29] introduced rough upper and lower surfaces made of pyramidal elements in a cylindrical cell. They found that these elements enhanced the production of plumes, which were directly injected into the core flow, leading to an increase in Nu. The increase in Nu was due to an increase in the pre-factor in the Nu–Ra scaling relation. Whereas subsequent experiments found no effect of periodic roughness on β [30–32], later studies confirmed that the changes in the flow field brought about by surface roughness do increase the value of β from the planar value [33–39]. In our previous study, we used roughness to break the top/bottom boundary layer symmetry, and found that a periodic upper surface with $\lambda_{\text{opt}} = 0.154$ maximized the heat transport with $\beta = 0.359$ for a smooth lower surface in high resolution numerical simulations [40]. As is the case with the present geometry, when $\lambda \ll \lambda_{\text{opt}}$ and $\lambda \gg \lambda_{\text{opt}}$, the planar results are recovered. For each Ra we determined the maximum Nu among all λ, thereby optimizing over all λ, to find $Nu_{\text{opt}} - 1 = 0.058 \times Ra^{0.334}$.

The first experimental attempt to use roughness to reach the ultimate regime at Ra accessible in the laboratory was made by Roche *et al.* [33], who used V-shaped grooves to cover the entire interior of their cylindrical cell of $\Gamma = 0.5$. They observed a transition in $Nu(Ra)$ at $Ra \approx 2 \times 10^{12}$, and that the data beyond the point of transition could be fit with a power law with $\beta = 0.51$. A similar transition was observed at $Ra = 7 \times 10^9$ in the simulations of Stringano *et al.* [35], who used a cylindrical geometry with V-shaped grooves at the upper and lower surfaces and imposed axisymmetry on the flow. This artificial symmetry had two important effects on the flow field: (1) The production and release of the plumes from the roughness elements was in tandem, resulting in larger plumes; and (2) The plumes traversed the vertical distance without encountering a large scale circulation in the interior region. Both these effects resulted in an increase in the efficiency of the heat transfer. As summarized by Ahlers et al., [41], it was first noted by Niemela & Sreenivasan [13] that the results of Roche *et al.* [33] can be understood as a transition between when the groove depth is less than the BL thickness to a regime where the groove depth is larger than the BL thickness. Ahlers et al., [41] state "More work is needed to resolve this issue." Here we present results from well resolved numerical simulations of Rayleigh-Bénard convection in a cell with rough upper and lower surfaces in two dimensions. The roughness profiles chosen are sinusoidal. By keeping the amplitude fixed and varying the wavelength of the rough surfaces, we study their effects on the heat transport.

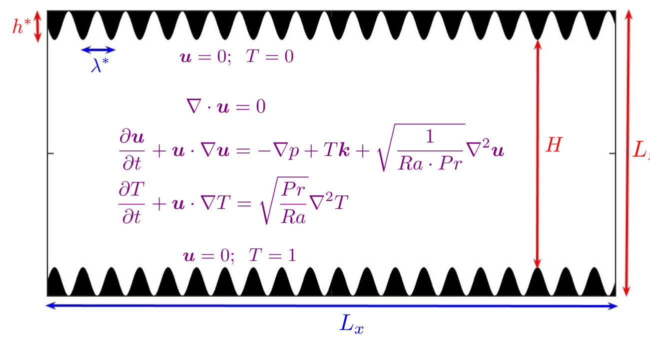

FIG. 1. The geometry of the rough surfaces and the equations of motion for our two-dimensional rectangular cell with $\Gamma = 2$.

The geometry and the dimensionless equations of motion studied here are shown in figure 1. The aspect ratio of the cell, $\Gamma \equiv L_x/L_z$, is fixed at 2. The rough surfaces have a wavelength $\lambda \equiv \lambda^*/L_z$ and an amplitude $h \equiv h^*/L_z$. The equations of motion for thermal convection are the Oberbeck-Boussinesq (O-B) equations [5], and are non-dimensionalized by choosing $H = L_z - 2h^*$ as the length scale and $U_0 = \sqrt{g\alpha\Delta T H}$ as the velocity scale. Hence, the time scale is $t_0 = H/U_0$. Here, $\boldsymbol{u}(\boldsymbol{x}, t) = (u(\boldsymbol{x}, t), w(\boldsymbol{x}, t))$ is the velocity field, $T(\boldsymbol{x}, t)$ is the temperature field, $\boldsymbol{k}$ is the unit vector along the vertical, and $p(\boldsymbol{x}, t)$ is the pressure field. No-slip and Dirichlet conditions for $\boldsymbol{u}$ and T are imposed on the rough surfaces, and periodic conditions are used in the horizontal.

The O-B equations were solved using the Lattice Boltzmann method with separate distributions for the momentum and temperature fields [42–46]. Our code has been extensively tested against results from numerical simulations for a wide range of different flows, and the details of the validation can be found in [40, 47].

For each of ten λ's (see Fig. 2) we simulated over the range $Ra = \left[4 \times 10^6, 3 \times 10^9\right]$. The planar wall case is $\lambda = 0$, the amplitude of the roughness is fixed at $h = 0.1$ and $Pr = 1$ for all simulations. We ran the simulations for at least $143\, t_0$, where t_0 is the turnover time, and statistics were collected only after $100\, t_0$. The Nusselt number was computed as

$$Nu = \frac{\left[-\kappa \frac{\partial \overline{T}}{\partial z} + \overline{wT}\right]_{z=z_e}}{\kappa \Delta T / H}, \tag{1}$$

where the overbar represents horizontal *and* temporal average. We should note here that this definition of Nu, in general, does not reduce to unity in the static case

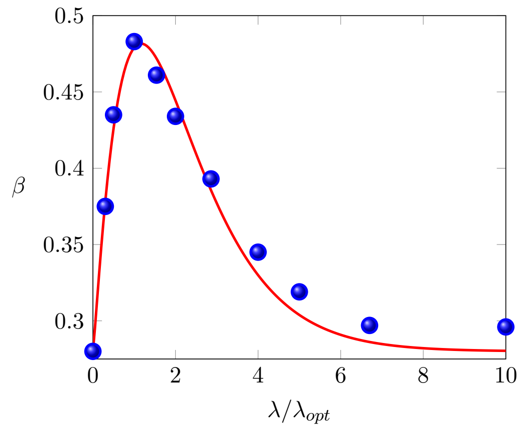

FIG. 2. The exponent in the scaling law $Nu - 1 = A \times Ra^{\beta}$ as a function of roughness wavelength λ (Here we used $\lambda =$ 0.03, 0.05, 0.1, 0.154, 0.2, 0.286, 0.4, 0.5, 0.67 and 1.0.) Data from simulations are the circles and the line is a fit using $\beta = 0.54\, x^{1.17}\, e^{-x} + 0.28$, where $x = \lambda/\lambda_{opt}$. At $\lambda_{\text{opt}} = 0.1$, we find a maximum $\beta_{\max} = 0.483$. For $\lambda = 1$, β is slightly larger than 0.28 because of finite-size effects. See also Fig. 2 of the Supplementary Material.

for arbitrary roughness geometries [1]; however, for the sinusoidal geometries used here this choice gives $Nu \approx 1$ when $Ra = 0$. To give an example of the spatial resolutions in the simulations, for $\lambda = 1$ and $Ra = 2 \times 10^9$ the number of grid points used are $N_x = 2800$ and $N_z = 1400$. Grid independence was ascertained from simulations at $Ra = 2 \times 10^9$ for $\lambda = 0.03$ and 0.2 using two grids: (a) $N_x = 2400$, $N_z = 1200$ and (b) $N_x = 2000$, $N_z = 1000$. The difference between Nu computed at $z_e = L_z/2$ for the two grids was less than 1.2%. As an additional check, Nu was computed at three different depths $z_e = L_z/4, L_z/2$, and $3\,L_z/4$; and the difference between Nu at any two depths was less than 0.5%. More simulation details are provided in the Supplementary Material.

For each λ, we obtained β from a linear least squares fit to the $Nu(Ra)$ simulation data. Figure 2 shows β in the scaling relation $Nu - 1 = A \times Ra^{\beta}$ as a function of λ. At the optimal wavelength $\lambda_{\text{opt}} = 0.1$, β attains a maximum value of 0.483, which indicates that the influence of BLs on heat transport has been minimized. It is clear that in the limits $\lambda \ll \lambda_{\text{opt}}$ and $\lambda \gg \lambda_{\text{opt}}$, the planar case is approached. The Nu-Ra scaling relations for different λ are shown in figure 3. The linear least-squares fit for $\lambda_{\text{opt}} = 0.1$ giving $Nu - 1 = 0.0042 \times Ra^{0.483}$ is shown in figure 3(a). The roughness elements are 'submerged' inside the thermal BLs for $Ra < 10^8$ (not shown), and hence, as seen in figure 3(b), the values of Nu for these Ra are close to those for larger λ. The increase in β for $\lambda = 0.1$ relative to other λ is clear from figure 3(b). Figure 3(b) also shows the fit obtained for $Nu_{\text{opt}}(Ra)$, which is obtained in the following manner:

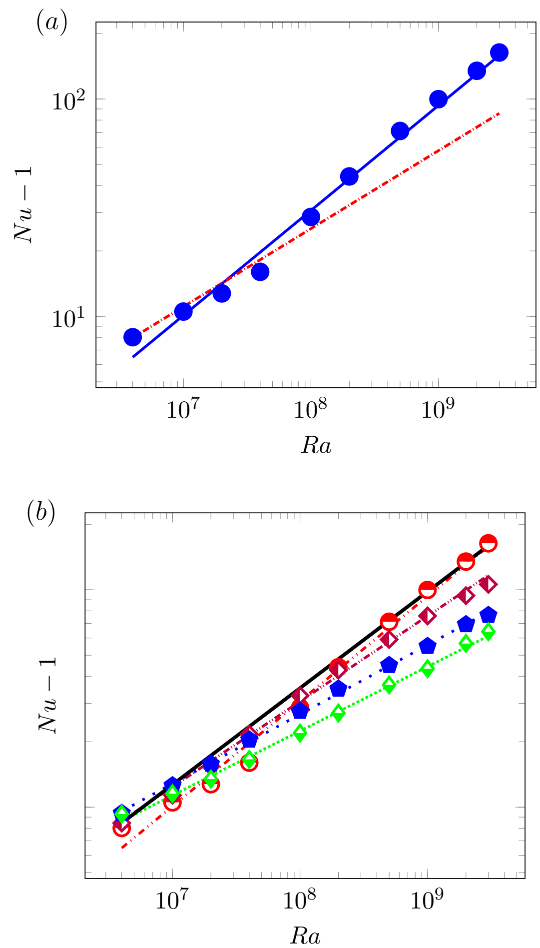

FIG. 3. Scaling relations for different λ. (a) Nu-Ra scaling relations for $\lambda = \lambda_{\text{opt}} = 0.1$. The linear least-squares fit is $Nu - 1 = 0.0043 \times Ra^{0.482}$. The dash-dotted line is the scaling fit $Nu - 1 = 0.034 \times Ra^{0.359}$ for single rough wall of $\lambda = 0.154$ [40]. (b) The (λ, β) pairs in the order of increasing slope are (1.0, 0.296), (0.5, 0.319), (0.286, 0.393), and (0.1, 0.482). The remaining pairs (not shown in figure 3(b)) are (0.03, 0.375), (0.05, 0.435), (0.154, 0.461), (0.2, 0.434), (0.4, 0.345), and (0.67, 0.297). The black line is the upper envelope is described by $Nu_{\text{opt}} - 1 = 0.01 \times Ra^{0.444}$. See also Figs. 1 and 2 of the Supplementary Material.

for each Ra we choose the maximum Nu among all λ, effectively optimizing over all λ. This data is described by $Nu_{\text{opt}} - 1 = 0.01 \times Ra^{0.444}$.

The flow field for the case of $\lambda_{\text{opt}} = 0.1$ and $Ra = 2 \times 10^9$ is shown in Fig. 4, where the following features are apparent:

1. Two large convection rolls in the cell interior.
2. The 'unstable' BLs at the upper and lower surfaces.
3. The production of plumes from the fluid moving along the rough surfaces and their ejection from the tips of the roughness elements.

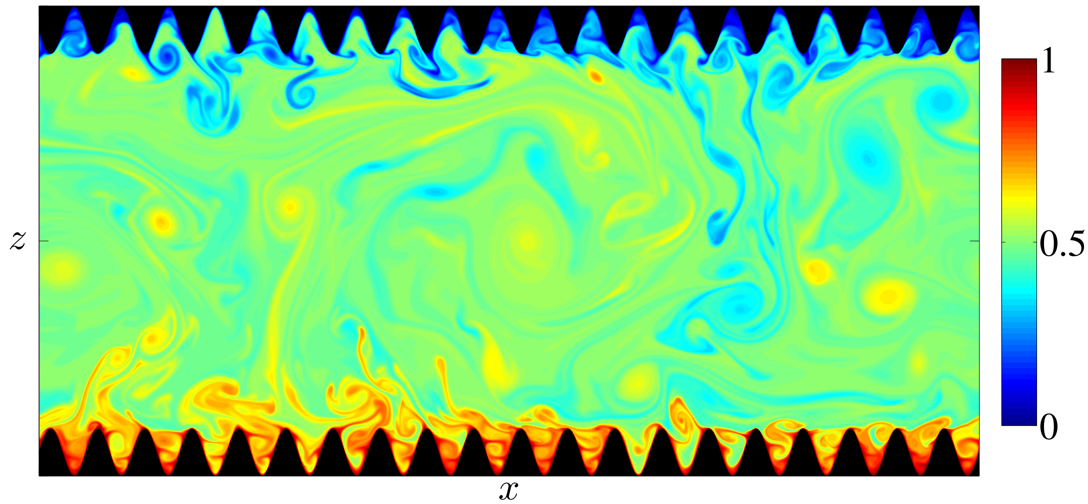

FIG. 4. A snapshot of the temperature field for $\lambda = 0.1$ and $Ra = 2 \times 10^9$. To see the effects of roughness, the flow field here can be contrasted with that in the smooth case studied by Johnston & Doering [28]. See also Fig. 3 of [40] which shows the transition from the planar to the rough flow field in the case of one rough wall.

By varying λ, we have achieved a state in which the interaction between the core flow and the BLs over the roughness elements has been enhanced. This results in an unstable state for the BLs, which then leads to the generation and ejection of plumes from the roughness tips. As noted above, in the case of a single rough wall, the maximum value of β was found to be $\beta \approx 0.36$ [40] but at a slightly larger λ. This highlights the role played by the second rough wall in further decreasing the role of the BLs in transporting heat. We should note here that in spite of the differences in geometry, our results have a correspondence with those of Waleffe *et al.* [25] and Sondak *et al.* [26] in that there is a length scale in each setting ($\lambda_{\rm opt}$ in ours and $\alpha_{\rm opt}$ in theirs) that optimizes heat transport. The optimization occurs through the manipulation of the coherent structures that transport heat, though in detail it is accomplished in different ways.

Our results are consistent with those of Goluskin & Doering [1], who used the background method to compute upper bounds [48] on Nu for R-B convection in a domain with rough upper and lower surfaces that have square-integrable gradients. They prove that $Nu \le C Ra^{1/2}$, where C depends on the geometry of roughness. Our results show that for the optimal wavelength the heat transport is $Nu - 1 = 0.0042 \times Ra^{0.483}$, with the value of C being four orders of magnitude larger than ours, but an exponent approaching their result. Importantly, their approach provides a key framework for exploring a range of amplitudes and wavelengths using our methodology. Finally, our findings demonstrate that the scaling of the ultimate regime is nearly achieved in two dimensions using rough walls. Roche *et al.* [33] interpreted their observation of $\beta = 1/2$ as being due to a laminar to turbulent transition of the BLs. Here, this state is achieved by the enhanced BL–core flow interaction driven by the roughness, which generates a larger number of intense plumes.

In summary, we have studied convection in a rectangular cell of $\Gamma = 2$ with rough upper and lower surfaces. At a fixed roughness amplitude, varying the wavelength λ results in a spectrum of exponents in the Nu-Ra scaling relation. At $\lambda_{\rm opt}$ the maximum exponent $\beta_{\rm max} = 0.483$ is achieved, and in the limits $\lambda \ll \lambda_{\rm opt}$ and $\lambda \gg \lambda_{\rm opt}$, the planar value of β is recovered, which may underlie why certain experiments found no effect of periodic roughness on β [30–32]. The observation of $\beta_{\rm max} \approx 0.5$ here has been facilitated by the use of very large amplitude roughness relative to existing studies [33, 35, 38], indicating the promise of examining this state experimentally for more moderate values of Ra than have been previously necessary. Indeed, by varying both amplitude and wavelength over a significant range, the systematic effects of the BLs, and thus the molecular properties of the fluid, may be realized, comparing and contrasting the concept of a laminar-to-turbulent BL transition, with the enhanced forcing associated with unstable BL's triggered by the roughness as seen here.

The authors acknowledge the support of the University of Oxford and Yale University, and the facilities and staff of the Yale University Faculty of Arts and Sciences High Performance Computing Center. S.T. acknowledges a NASA Graduate Research Fellowship. J.S.W. acknowledges NASA Grant NNH13ZDA001N-CRYO, Swedish Research Council grant no. 638-2013-9243, and a Royal Society Wolfson Research Merit Award for support.

* john.wettlaufer@yale.edu

[1] D. Goluskin and C. R. Doering, J. Fluid Mech. **804**, 370 (2016).
[2] L. P. Kadanoff, Phys. Today **54**, 34 (2001).
[3] M. G. Worster, in *Perspectives in Fluid Dynamics — a Collective Introduction to Current Research*, edited by G. Batchelor, H. Moffatt, and M. Worster (Cambridge University Press, 2000) pp. 393 – 446.
[4] J. S. Wettlaufer, Phys. Today **64**, 66 (2011).
[5] S. Chandrasekhar, *Hydrodynamic and Hydromagnetic Stability* (Dover Publications, 2013).
[6] C. Priestley, Austr. J. Phys. **7**, 176 (1954).
[7] W. V. R. Malkus, Proc. R. Soc. Lond. A **225**, 196 (1954).
[8] L. N. Howard, in *Applied Mechanics, Proc. of the 11th Congr. of Appl. Mech. Munich (Germany)*, edited by H. Görtler (Springer, 1966) pp. 1109–1115.
[9] R. H. Kraichnan, Phys. Fluids **5**, 1374 (1962).
[10] E. A. Spiegel, Annu. Rev. Astron. Astrophys. **9**, 323 (1971).
[11] S. Grossmann and D. Lohse, J. Fluid Mech. **407**, 27 (2000).
[12] J. Niemela, L. Skrbek, K. R. Sreenivasan, and R. J. Donnelly, Nature **404**, 837 (2000).
[13] J. Niemela and K. R. Sreenivasan, J. Fluid Mech. **557**, 411 (2006).
[14] P. Urban, V. Musilová, and L. Skrbek, Phys. Rev. Lett. **107**, 014302 (2011).
[15] P. Urban, P. Hanzelka, T. Kralik, V. Musilova, A. Srnka, and L. Skrbek, Phys. Rev. Lett. **109**, 154301 (2012).
[16] R. Verzicco and R. Camussi, J. Fluid Mech. **477**, 19 (2003).
[17] R. J. Stevens, D. Lohse, and R. Verzicco, J. Fluid Mech. **688**, 31 (2011).
[18] B. Gayen, G. O. Hughes, and R. W. Griffiths, Phys. Rev. Lett. **111**, 124301 (2013).
[19] X. Chavanne, F. Chilla, B. Castaing, B. Hebral, B. Chabaud, and J. Chaussy, Phys. Rev. Lett. **79**, 3648 (1997).
[20] X. He, D. Funfschilling, H. Nobach, E. Bodenschatz, and G. Ahlers, Phys. Rev. Lett. **108**, 024502 (2012).
[21] L. Skrbek and P. Urban, J. Fluid Mech. **785**, 270 (2015).
[22] Z. He, E. Bodenschatz, and G. Ahlers, J. Fluid Mech. **791**, R3 (2016).
[23] V. Borue and S. A. Orszag, J. Sci. Comp. **12**, 305 (1997).
[24] D. Lohse and F. Toschi, Phys. Rev. Lett. **90**, 034502 (2003).
[25] F. Waleffe, A. Boonkasame, and L. M. Smith, Phys. Fluids **27**, 051702 (2015).
[26] D. Sondak, L. M. Smith, and F. Waleffe, J. Fluid Mech. **784**, 565 (2015).
[27] J. Schmalzl, M. Breuer, and U. Hansen, Europhys. Lett. **67**, 390 (2004).
[28] H. Johnston and C. R. Doering, Phys. Rev. Lett. **102**, 064501 (2009).
[29] Y. Shen, P. Tong, and K.-Q. Xia, Phys. Rev. Lett. **76**, 908 (1996).
[30] Y.-B. Du and P. Tong, Phys. Rev. Lett. **81**, 987 (1998).
[31] Y.-B. Du and P. Tong, J. Fluid Mech. **407**, 57 (2000).
[32] S. Ciliberto and C. Laroche, Phys. Rev. Lett. **82**, 3998 (1999).
[33] P.-E. Roche, B. Castaing, B. Chabaud, and B. Hébral, Phys. Rev. E **63**, 045303 (2001).
[34] X.-L. Qiu, K.-Q. Xia, and P. Tong, J. Turb. **6**, 1 (2005).
[35] G. Stringano, G. Pascazio, and R. Verzicco, J. Fluid Mech. **557**, 307 (2006).
[36] J.-C. Tisserand, M. Creyssels, Y. Gasteuil, H. Pabiou, M. Gibert, B. Castaing, and F. Chilla, Phys. Fluids **23**, 015105 (2011).
[37] J. Salort, O. Liot, E. Rusaouen, F. Seychelles, J.-C. Tisserand, M. Creyssels, B. Castaing, and F. Chilla, Phys. Fluids **26**, 015112 (2014).
[38] P. Wei, T.-S. Chan, R. Ni, X.-Z. Zhao, and K.-Q. Xia, J. Fluid Mech. **740**, 28 (2014).
[39] S. Wagner and O. Shishkina, J. Fluid Mech. **763**, 109 (2015).
[40] S. Toppaladoddi, S. Succi, and J. S. Wettlaufer, EPL **111**, 44005 (2015).
[41] G. Ahlers, S. Grossmann, and D. Lohse, Rev. Mod. Phys. **81**, 503 (2009).
[42] R. Benzi, S. Succi, and M. Vergassola, Phys. Rep. **222**, 145 (1992).
[43] F. Massaioli, R. Benzi, and S. Succi, Europhys. Lett. **21**, 305 (1993).
[44] S. Chen and G. D. Doolen, Ann. Rev. Fluid Mech. **30**, 329 (1998).
[45] X. Shan, Phys. Rev. E **55**, 2780 (1997).
[46] Z. Guo, C. Zheng, and B. Shi, Phys. Rev. E **65**, 046308 (2002).
[47] S. Toppaladoddi, S. Succi, and J. S. Wettlaufer, Procedia IUTAM **15**, 34 (2015).
[48] A detailed discussion of upper-bound studies can be found in Kerswell [49] and Hassanzadeh *et al.* [50].
[49] R. R. Kerswell, Physica D **121**, 175 (1998).
[50] P. Hassanzadeh, G. P. Chini, and C. R. Doering, J. Fluid Mech. **751**, 627 (2014).